1521-0111/12/8203-521–528$25.00
MOLECULAR PHARMACOLOGY
Vol. 82, No. 3
77248/3791305

Mol Pharmacol 82:521–528, 2012

Transcriptome Analysis and In Vivo Activity of Fluvastatin versus Zoledronic Acid in a Murine Breast Cancer Metastasis Model[S]

Nadejda Vintonenko, Jean-Philippe Jais, Nadim Kassis, Mohamed Abdelkarim, Gerard-Yves Perret, Marc Lecouvey, Michel Crepin, and Melanie Di Benedetto

Unité Mixte de Recherche 7244 Centre National de la Recherche Scientifique, Chimie, Structure et Propriétés de Biomatériaux et d'Agents Thérapeutiques, Université Paris 13, Bobigny, France (N.V., M.A., M.L., M.D.B.); Institut National de la Santé et de la Recherche Médicale, 553 Endothélium et Angiogénèse Laboratoire d'Hémostase, Paris, France (N.V., M.C.); Service de Biostatistique et Informatique Médicale, Hôpital Necker, Université Paris Descartes, Paris, France (J.-P.J.); Laboratory of Homeostasie Energetique et Regulation Endocrine et Nerveuse, Functional and Adaptive Biology Unit-Centre National de la Recherche Scientifique Équipes d'Accueil Conventionnées4413, University Paris-Diderot, Paris, France (N.K.); Université Paris 13, EA4222, Laboratory of Immunology and Immunopathology, Bobigny, France (G.-Y.P.); Université Paris 7, Unité Mixte de Recherche Scientifique 940, Institut de Génétique Moléculaire Paris, France (M.D.B.)

Received February 6, 2012; accepted June 20, 2012

ABSTRACT

Statins and bisphosphonates are two distinct classes of isoprenoid pathway inhibitors targeting downstream enzyme to HMG-CoA reductase (upstream enzyme) and farnesyl-pyrophosphate synthase, respectively. Here, we studied fluvastatin (Fluva) and zoledronate (Zol), representative molecules of each class, respectively. In vivo metastatic potentials of both molecules were assessed. For the first time, we observed a significant reduction in progression of established metastases with Fluva treatment. Treatment with both Zol at 100 μg/kg and Fluva at 15 mg/kg inhibited 80% of the metastasis bioluminescence signal and increased survival of mice. The Zol and Fluva transcriptomic profiles of treated MDA-MB-231 cells revealed analogous patterns of affected genes, but each of them reached with different kinetics. The observable changes in gene expression started after 24 h for Fluva $IC_{50\ 72\ h}$ and only after 48 h for Zol $IC_{50\ 72\ h}$. To obtain early changes in gene expression of Zol-treated cells, a 3 times higher dose of Zol $IC_{50\ 72\ h}$ had to be applied. Combining Fluva and Zol in vivo showed no synergy, but a benefit of several days in survival of mice. This study demonstrated that Zol or Fluva is of potential clinical use for the treatment of established metastasis.

Introduction

Breast cancers are frequently characterized by overexpression of Rho family GTPases and constitutive activation of Ras or other small GTP-binding proteins that are mutated in a variety of tumors, thereby regulating cancer cell migration and invasion (Fritz et al., 1999). To be functional, these proteins require prenylation, a lipid post-translational modification that assures their translocation and attachment to the plasma membrane crucial for their ultimate involvement in signal transduction. In human cells, isoprenoids (farnesyl-pyrophosphate and geranylgeranyl-pyrophosphate) are derived from the mevalonate pathway that starts from the reaction of conversion of HMG-CoA to mevalonic acid catalyzed by HMG-CoA reductase (the rate-limiting reaction in cholesterol biosynthesis). Evidence has been accumulating on the direct inhibitory effects of bisphosphonates (BPs) and statins, initially known as potent inhibitors of osteoclast-mediated bone resorption and cholesterol-lowering drugs, respectively, on cancer progression and metastasis (Fig. 1).

Use of bisphosphonates (Russell, 2011) in solid tumors to prevent or treat bone metastases is supported by numerous clinical studies and is recommended by international consensus conferences (Aapro et al., 2008). The effects of bisphosphonates on soft tissue metastases are less clear (Fournier et al., 2010) Moreover, recent studies show that zoledronic acid (Zometa, Zol) could induce adverse cytotoxic effects such as

This work was supported by "La Ligue nationale contre le cancer Comité Ile-de France" [7FI9633JSVN] and the Institut National contre le Cancer [PL06_130].

Article, publication date, and citation information can be found at http://molpharm.aspetjournals.org.

http://dx.doi.org/10.1124/mol.111.077248.

[S] The online version of this article (available at http://molpharm.aspetjournals.org) contains supplemental material.

ABBREVIATIONS: BP, bisphosphonate; Zol, zoledronate; NBP, aminobisphosphonate; Fluva, fluvastatin; PBS, phosphate-buffered saline; PCR, polymerase chain reaction; BP7033, 1-benzyl-1 hydroxymethylene-1,1 bisphosphonic acid; ANOVA, analysis of variance.

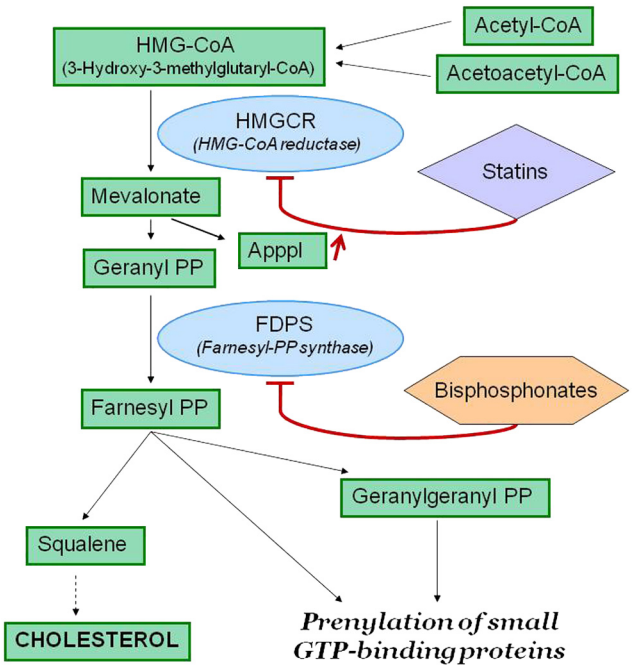

Fig. 1. Mevalonate pathway inhibition scheme. Prenylation of small G-proteins can be inhibited either by statins acting on upstream enzyme HMG-CoA reductase or by bisphosphonates targeting downstream enzyme farnesyl-pyrophosphate synthase, which could lead to accumulation of the cytotoxic ATP analog ApppI.

osteonecrosis of the jaw. This effect could be bypassed using Zol in combination with other chemotherapeutic molecules. Zol, the more potent drug among the aminobisphosphonates (NBPs), is described to suppress prenylation of several intracellular small GTPases essential for many cellular functions important in carcinogenesis (Caraglia et al., 2006). However, the inhibition of breast cancer cell proliferation by NBPs, including Zol, seems to involve other mechanisms besides the inhibition of the mevalonate pathway because none of the mevalonate pathway intermediates completely reversed the effect of NBPs on MDA-MB-231 proliferation (Reinholz et al., 2002). On the other hand, 1-benzyl-1 hydroxymethylene-1,1 bisphosphonic acid, a novel non–nitrogen-containing BP (BP7033) has been shown to prevent post-translational Ras processing similarly to NBPs (Hamma-Kourbali et al., 2003). In addition, Zol has been found to induce formation of a novel adenine nucleotide translocase-inhibiting cytotoxic ATP analog, ApppI. Thus, Zol could act on cell apoptosis both via inhibition of the mevalonate pathway and by the blockage of mitochondrial adenine nucleotide translocase (Mönkkönen et al., 2006). Zol has been demonstrated to inhibit proliferation and induce apoptosis (Jagdev et al., 2001; Senaratne et al., 2002), inhibit cell invasion (Denoyelle et al., 2003), and potently diminish bone and also visceral metastasis in vivo (Green et al., 2000; Peyruchaud et al., 2001; Hiraga et al., 2004; Duivenvoorden et al., 2007). In addition, accumulating evidence indicates that bisphosphonates antitumor effects could be potentiated by other chemotherapeutic drugs (Yano et al., 2003). Several cases of possible synergy between bisphosphonates and statins or other mevalonate pathway inhibitors in vitro (Budman and Calabro, 2006; Issat et al., 2007; Dudakovic et al., 2008) and in vivo (Issat et al., 2007) showing potentiated effects have been reported.

Fluvastatin (Lescol, Fluva) represents lipophilic statins able to directly cross cell membranes in contrast to hydrophilic statins, such as pravastatin, unable to penetrate membrane lipid bilayers (Istvan, 2003). Of interest, results from epidemiological studies concur on the protective effects of lipophilic statins on breast cancer risk (Cauley et al., 2006; Ahern et al., 2011). In breast cancer cells, Fluva was shown to exert significant growth inhibitory activity (Campbell et al., 2006) and reduce transendothelial migration of MDA-MB-231 cells in correlation with the inhibition of the membrane localization of RhoA and RhoC, but not with Ras (Kusama et al., 2006).

Fluva and Zol are used to treat and prevent atherosclerosis and osteoporosis, respectively, mainly in elderly individuals at an age when the prevalence of cancers increases sharply. Both drugs are therefore often coprescribed in patients with cancer, and they might influence the progression of the disease (Jadhav and Jain, 2006). Because the potential effects of Fluva in vivo on breast cancer established metastases have not been described yet and because statins and bisphosphonates are frequently coadministered, we wanted to investigate the effects of these drugs using in vivo imaging system with a highly invasive bioluminescent MDA-MB-231 breast cancer subpopulation characterized by oncogenic *KRAS* mutation (Kozma et al., 1987) and constitutive activation of Ras as well as overexpression of RhoA (Fritz et al., 1999). Furthermore, because BPs induce apoptosis by forming ATP analogs (ApppI) that could be complementary to the fluvastatin inhibition effect involving small G proteins, we also evaluated the combination of these two drugs on established MDA-MB-231 metastases (Fig. 1).

Materials and Methods

Cell Culture and Drugs. The human breast adenocarcinoma MDA-MB-231 cells, obtained from the American Type Culture Collection (Manassas, VA), were maintained in Dulbecco's minimal essential medium supplemented with 10% fetal bovine serum, 1% sodium pyruvate, and antibiotics (1% penicillin sodium and 1% streptomycin) at 37°C in a humidified atmosphere containing 5% carbon dioxide. the D3H2LN cell line isolated from MDA-MB-231 lymph node metastasis was purchased from Caliper Life Sciences (Alameda, CA). The D3H2LN cell line was a clone selected from a MDA-MB-231 stable clone expressing luciferase. MDA-MB-231 cells expressing luciferase were injected into the mammary fad pad of nude mice and after 12 weeks of growth in vivo, they were harvested and repropagated in vitro. This subclone was injected once more into the mammary fad pad of mice to yield a second D3H2LN cell line, harvested from a lymph node metastasis (Jenkins et al., 2005). D3H2LN cells were cultured in minimum essential medium with Earl's balanced salts solution supplemented with 10% fetal bovine serum, 1% nonessential amino acids, 1% L-glutamine, and 1% sodium pyruvate and antibiotics (all from HyClone, Logan, UT) at 37°C in a humidified atmosphere containing 5% carbon dioxide.

Fluvastatin was purchased from (Axxora, Coger S.A.R.L., Paris, France). Zol was synthesized as described earlier (Lecouvey et al., 2001; Monteil et al., 2005).

In Vitro Viability Inhibition Assay. MDA-MB-231 and D3H2LN cell viability was assessed using the 3-(4,5-dimethylthiazol-2-yl)-2,5-diphenyltetrazolium-microculture tetrazolium assay (Mosmann, 1983). The cells (5000 cells/well in a 96-well plate) were then incubated with different concentrations of Zol or Fluva for 24, 48, and 72 h at 37°C in a 5% CO_2 incubator. Optical density was measured at 570 nm using a Labsystems Multiskan MS microplate reader.

Intracardiac Experimental Metastasis Model. Fluva and Zol effects were evaluated on already established metastasis. A Zol dose of 100 μg/kg, corresponding to 2.5 μg/mouse, was chosen to be inferior to the effective dose described earlier in the 4T1/luc mouse breast cancer model (5 μg/mouse; i.e., 150–200 μg/kg) (Hiraga et al., 2004). The highest Fluva dose (15 mg/kg/day), equivalent to a human dose of 80 mg/day, was chosen according to previous publication (Campbell et al., 2006). Drug curative effects on the progression of established metastases were evaluated as follows. Female nude mice, 8 to 10 weeks old (Janvier, Le Genest St. Isle, France), were anesthetized intraperitoneally with 120 mg/kg ketamine and 6 mg/kg xylazine and were injected with D3H2LN (1×10^5cells) in 100 μl of sterile PBS into the left ventricle of the heart by nonsurgical means. A successful intracardiac injection was immediately confirmed by a systemic bioluminescence signal distributed throughout the animal. Only mice with satisfactory injection continued the experiment. Once metastatic colonization had been confirmed 7 to 10 days after cells intracardiac injection (the baseline of the metastasis bioluminescent signal was set to 300 photon counts/s maintained for 2 to 3 days; i.e., seen at two subsequent acquisitions), treatments were administered by intraperitoneal injection with 100 μl of PBS solutions with Zol (100 μg/kg three times a week) or Fluva (1 or 15 mg/kg daily) or PBS alone (daily for the control group). The first day of drug administration was denoted as day 0, and the treatments lasted for 3 weeks (day 21).

Bioluminescent Imaging. Mice Anesthetized by exposure to 1 to 3% isoflurane were placed in the IVIS Imaging System (Xenogen Corporation, Alameda, CA) and imaged from both dorsal and ventral views approximately 5 min after intraperitoneal injection of 150 μl of D-luciferin (Caliper Life Sciences) at 30 mg/ml per mouse. Assessment of established metastasis was evaluated by imaging during the treatment period (3 weeks). Acquisition time was 5 min at the beginning of the time course and was progressively reduced afterward in accordance with signal strength to avoid saturation. Analysis was performed using Living Image software (Xenogen Corporation) by measurement of photon flux (photon per second per square centimeter) with a region of interest drawn around the whole-animal bioluminescence signal. Signals of both dorsal and ventral views at early stages and from four views (dorsal, ventral, left, and right) at later stages were averaged for each animal to avoid the discrepancy related to the depth of metastases location.

Gene Expression Profiling. MDA-MB-321 cells were lysed after 12 and 24 h of treatment with 2 μM fluvastatin or 30 μM zoledronate [concentrations corresponding to IC_{50} at 72 h of treatment ($IC_{50\ 72\ h}$)] or after treatment with zoledronate for a longer time (48 h at 30 μM) or at a higher concentration (24 h at 100 μM zoledronate). Controls were treated with an equivalent volume of 1× PBS added to each drug solution. Total RNA from these treated or control cell cultures (four independent replicates for each condition) were isolated using an RNeasy Mini Kit (QIAGEN, Valencia, CA) by direct lyses on the 10-cm culture dish with 600 μl of RLT buffer, following the manufacturer's instructions. Purified RNA was quantified with a NanoDrop ND-1000 spectrophotometer (Thermo Fisher Scientific, Waltham, MA), and its quality was checked by running the Eukaryotic Total RNA Nano Assay in a Bioanalyzer 2100 (Agilent Technologies, Santa Clara, CA) using an Agilent RNA 6000 Nano Kit. Samples were prepared for hybridization to Affymetrix GeneChip Human Gene 1.0 ST arrays according to the manufacturer's instructions starting from 300 ng of total RNAs. Quality control of cRNA synthesis, hybridization, and data acquisition was performed according to the manufacturer's protocol and completed with personal quality control and data visualization.

Data Analysis. Raw data were processed with the apt-probeset-summarize program from Affymetrix Power Tools (version 1.10.2) for background correction and normalization. The RMA (robust multi-chip analysis) algorithm (Irizarry et al., 2003) with full quantile normalization was applied using the array design library files (V1 release 4), and normalized values were expressed on a log base 2 scale. Transcripts and genes were annotated with Affymetrix release 29 annotation files based on the human genome version 18 assemblies. Data analysis was performed with the R Bioconductor LIMMA package. The microarray data have been deposited in the National Center for Biotechnology Information Gene Expression Omnibus (Edgar et al., 2002) and are accessible through Gene Expression Omnibus series accession number GSE33552 (http://www.ncbi.nlm.nih.gov/geo/query/acc.cgi?acc=GSE33552). Probe sets corresponding to control genes or having a low-intensity signal (median log 2 of intensity <4) or low variability (trimmed range excluding the minimum-maximum values <0.5) were not considered for further analyses, yielding a total of 22,289 probe sets. Only genes with a false discovery rate <0.05 and fold change ≥1.5 in paired comparison between treatments and their corresponding controls were considered as differentially regulated. Analysis of genes associated with cell functions was performed using Ingenuity Pathways Analysis software (Ingenuity Systems, Redwood City, CA) to identify biological processes and pathways that may be associated with modulated gene expression.

Quantitative Real-Time Reverse Transcriptase-PCR Analysis. Total RNA (20 μg) was reverse-transcribed using M-MLV reverse transcriptase (Invitrogen, Carlsbad, CA) and random primers from Roche Applied Science (Indianapolis, IN); 40 ng of reverse-transcribed RNA was used as template for each reaction. Quantitative PCR assays were designed using Universal Probe Library site (https://www.roche-applied-science.com/sis/rtpcr/upl/index.jsp; Roche Applied Science). Real-time PCR was performed on a LightCycler 1.5 Real-Time PCR System (Roche Applied Science) using either a LightCycler FastStart DNA Master^{PLUS} SYBR Green I Kit with primers purchased from TIB MOLBIOL Syntheselabor GmbH (Berlin, Germany) or a LightCycler TaqMan Master Kit and Universal Probe Library probes with primers from TIB MOLBIOL. The reactions were cycled 45 times (95°C, 10 s; 60°C, 30 s) after an initial 10-min incubation at 95°C for the TaqMan procedure or 95°C for 10 min, followed by 45 cycles of 95°C for 10 s, 60°C for 10 s, and 72°C for 10 s for the SYBR Green procedure. Results were normalized to the expression of *PPia* or *beta2M*, two genes that exhibit little variation in this data set of the five housekeeping genes tested. Similar results were obtained for both genes of reference. The mRNA transcript level for target genes was calculated as outlined previously (Pfaffl et al., 2002): Ratio = $(\text{Eff target})^{\Delta Cp\ \text{insulin}(\text{MEAN control} - \text{MEAN sample})}/(\text{Eff reference})^{\Delta Cp\ 18S(\text{MEAN control} - \text{MEAN sample})}$.

Statistical Analysis. Analysis of in vitro and in vivo metastasis progression (bioluminescent signal or number of metastatic sites) was performed using the ANOVA Tukey-Kramer multiple comparisons test and Student's t test. $P < 0.05$ was considered significant. Kaplan-Meyer survival curves were generated using GraphPad Prism software (GraphPad Software Inc., San Diego, CA).

Results

In Vivo Antimetastatic Potential of Zol and Fluva. The drug effect on the progression of established metastases was evaluated (Figs. 2 and 3). Mice with successful intracardiac injections (Fig. 2A) developed metastases within 2 weeks. Once metastasis was detected (bioluminescent signal >300 photon counts), mice were randomly divided into four groups and received intraperitoneal injections three times per week with Zol at 100 μg/kg ($n = 8$) or daily with Fluva at 1 mg/kg ($n = 8$) or 15 mg/kg ($n = 7$) or were treated daily with PBS for the control group ($n = 8$) during 3 weeks. Although no significant effect on metastasis bioluminescence was observed with Fluva at 1 mg/kg (Supplemental Fig. S1), treatment with Fluva at 15 mg/kg or Zol at 100 μg/kg induced approximately 80% inhibition of luminescence signaling at the end of treatment ($P = 0.01$ and $P = 0.02$, respectively)

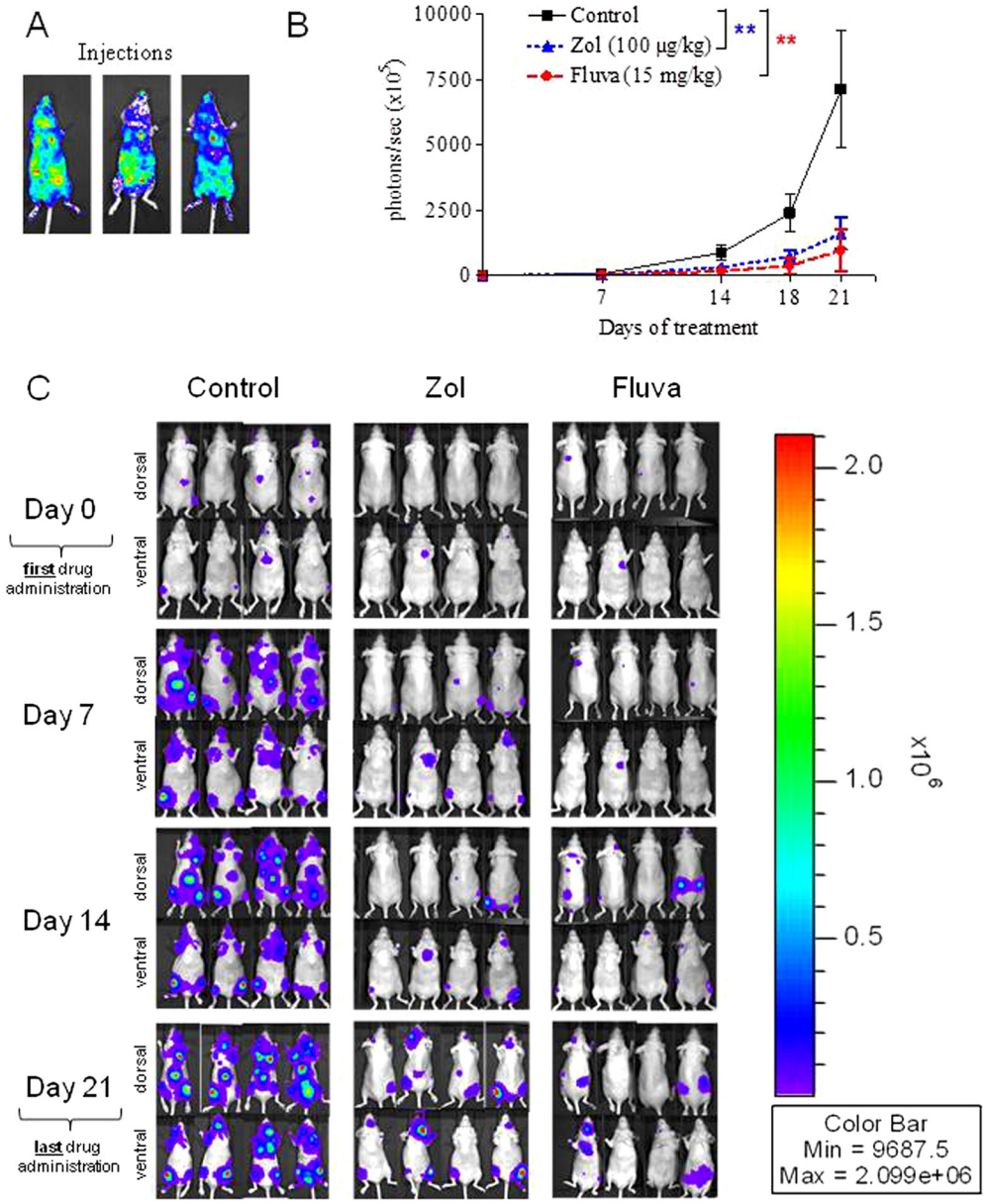

Fig. 2. Fluvastatin or zoledronate alone reduces the metastatic burden in a breast cancer metastasis mouse model. A, bioluminescent MDA-MB-231 (D3H2LN) cells (10^5) were injected into the left ventricle of nude mice. Only mice with successful intracardiac injection of cells, witnessed by an overall luminescent signal, continued the experiment. B, plot of bioluminescent signal for the control mice (treated daily with 1× PBS) and mice treated with Zol (at 100 μg/kg three times a week) and Fluva (at 15 mg/kg daily); each point represents a mean (± S.E.M.) signal of eight (Control or Zol) or seven (Fluva) mice. **, $P < 0.01$ versus control (ANOVA Tukey-Kramer multiple comparisons test for day 21 control, Zol, and Fluva). C, treatment with Zol, Fluva, or PBS for the control group was started upon confirmation of detectable established metastasis within 2 weeks after injections (denoted as day 0 for treatment); representative bioluminescent images for the indicated days of treatment are rendered at the same photon scale for the control group and for mice treated with Zol (100 μg/kg) and Fluva (15 mg/kg).

(Fig. 2, B and C). During the last (3rd) week of treatment, three of seven Fluva-treated (15 mg/kg) mice manifested a decrease in established metastatic sites, and five of seven mice showed a visibly reduced/stabilized bioluminescent signal (Fig. 3A; Supplemental Table 1); this decrease in metastasis luminescence was not observed with Zol.

To visualize the organs affected by metastases, we performed ex vivo analysis. Ex vivo imaging of the different tissues after the final imaging in vivo showed bone lesions (legs, scull, and spine) as well as ovary, brain, lung, kidney, and lymph node lesions (Fig. 3B).

Mice survival curves were generated from the first drug administration, followed by the 3-week-treatment, until they died (Fig. 3C). Fluva (15 mg/kg) or Zol (100 μg/kg) treatment significantly reduced the death of mice compared with control mice with median survival of 21 days for control mice, 33 for Zol treatment, and 28 for Fluva treatment ($P = 0.0245$) (Fig. 3C).

Transcriptomic Profiling of Zol or Fluva. To evaluate the different genes regulated by Zol and Fluva, we performed a transcriptomic analysis. To find a comparable treatment condition for each drug, their effects on MDA-MB-231 breast cancer cells survival/proliferation were first tested using a standard 3-(4,5-dimethylthiazol-2-yl)-2,5-diphenyltetrazolium assay at 12, 24, 48, and 72 h (Supplemental Fig. S2). Initially, we chose the concentration as the half-maximal inhibitory concentration detected after 72 h of treatment ($IC_{50\ 72\ h}$), corresponding to 2 μM for fluvastatin and 30 μM for zoledronate. Early treatment was chosen (12 and 24 h). RNAs extracted from four replicates (four independent treatments and respective controls for each condition) at each time point were subjected to hybridization on HuGene 1.0ST Affymetrix arrays (Fig. 4). Analysis of gene functions common to Zol and Fluva (540 probe sets: 373 up- and 167 down-regulated annotated genes; Supplementary Table 4, A and B) showed that the majority of them were involved in

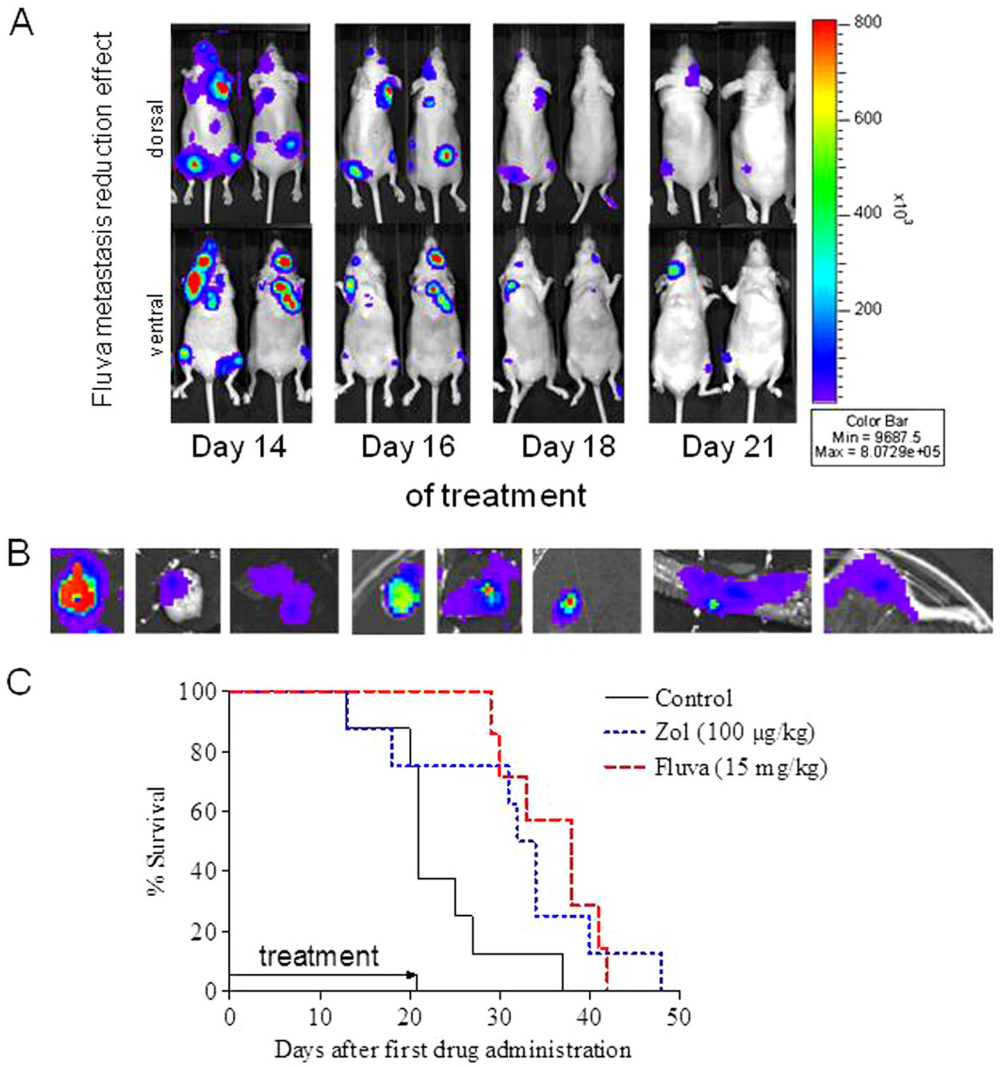

Fig. 3. Effects of Fluva on number of metastatic sites and survival of mice. A, number of detected metastatic sites in Fluva (15 mg/kg)-treated and control mice. The duration of treatment was 21 days. *B,* ex vivo representative images of metastatic sites in mice treated with Fluva (15 mg/kg). *C,* Kaplan-Meyer survival curves for control, Zol (100 μg/kg)-treated, and Fluva (15 mg/kg)-treated mice (median survival of 21, 33, and 38 days, respectively) generated for the 3-week treatment period and followed up until they died.

functions critical for metastatic steps such as cellular proliferation, migration, invasion, and apoptosis (Fig. 4, A and B). In addition, only nine genes (*DKK1*, *FGF1*, *FST*, *G0S2*, *HIF1A*, *LGALS3*, *PVR*, *TNFRSF12*, and *UAP1*) depending on Ras activation were modified compared with previous work (Loboda et al., 2010). In addition, by compiling genes whose expression is dependent on mitogen-activated protein kinase/phosphatidylinositol 3-kinase pathways as described in a previous publication (Bild et al., 2006), only 9% of the genes whose expression depends on prenylation of Ras protein or Rho activation were modified. Transcriptomic data were validated by quantitative PCR on 13 genes differentially regulated by Zol or Fluva (5 Zol-specific and 8 common Zol/Fluva genes indicated by asterisks in Supplemental Tables 3 and 4).

The analysis of genes that showed significantly different expression in a comparison of treated and control cells (false discovery rate <0.05, fold change >1.5) revealed 29 probe sets (18 + 11 on the diagram) for Fluva at 12 h, an additional 526 probe sets for Fluva at 24 h (16 + 365 + 145 on the diagram) (Supplemental Fig. S3A), and no significant genes for Zol at 12 or at 24 h (Supplemental Fig. S3B). Analysis of genes specifically regulated by each drug revealed 16 probe sets for Fluva corresponding to 12 annotated genes (Supplemental Figure S3, A and C; Supplemental Table 2) and a larger number (1032 probe sets corresponding to 951 annotated genes) for Zol treatments (Supplemental Fig. S3, A and D; Supplemental Table 3). The majority of genes regulated by Fluva at 12 or 24 h (100 and 97%, respectively) were common to the Zol 100 mg/kg at 24-h (Zol100 24h) gene profile (Supplemental Fig. S3A). Clustering of common Fluva and Zol genes (Supplemental Fig. S3B) reveals that for Zol treatment the pattern starts to appear at 24 h with the shortest distance found between Zol at 48 h (ZOLCONT48) and Fluva at 12 h (FLUVACONT12) indicating early changes. It might indicate retarded Zol kinetics because changes induced by Zol at 48 h were most similar to those induced by Fluva at 12 h.

In Vivo Antimetastatic Potential of Zol and Fluva Combination. Because Zol inhibited apoptosis differently from Fluva by inducing the cytotoxic analog ApppI (Fig. 1) and because the combination of these two drugs was also reported to be synergistic in vitro (Budman and Calabro, 2006), we tested the combination treatment in vivo using the same concentrations as described above for these drugs alone. Mice were treated with Zol (100 μg/kg, three times a week) combined with Fluva at 1 or 15 mg/kg administered daily (Supplemental Fig. S1; Fig. 5). The combination of Zol

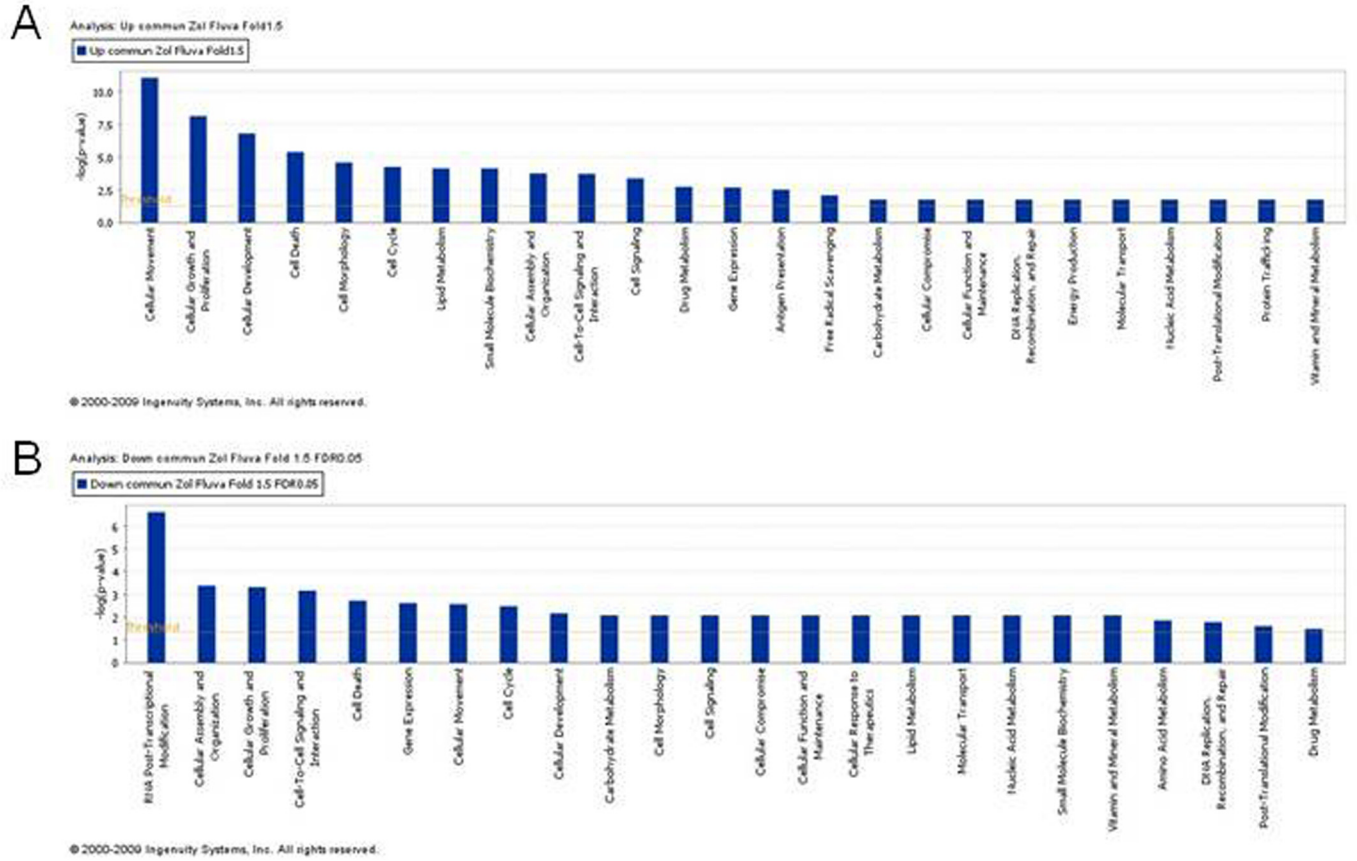

Fig. 4. Functional analysis of genes commonly regulated by Fluva or Zol. Ingenuity Pathways Analysis for 540 probe sets common between Fluva (either at 12 or 24 h) and Zol (either at 30 μM at 48 h or 100 μM at 24 h) treatments. A, 373 up-regulated probe sets corresponding to 370 annotated genes. B, 167 down-regulated probe sets corresponding to 166 annotated genes.

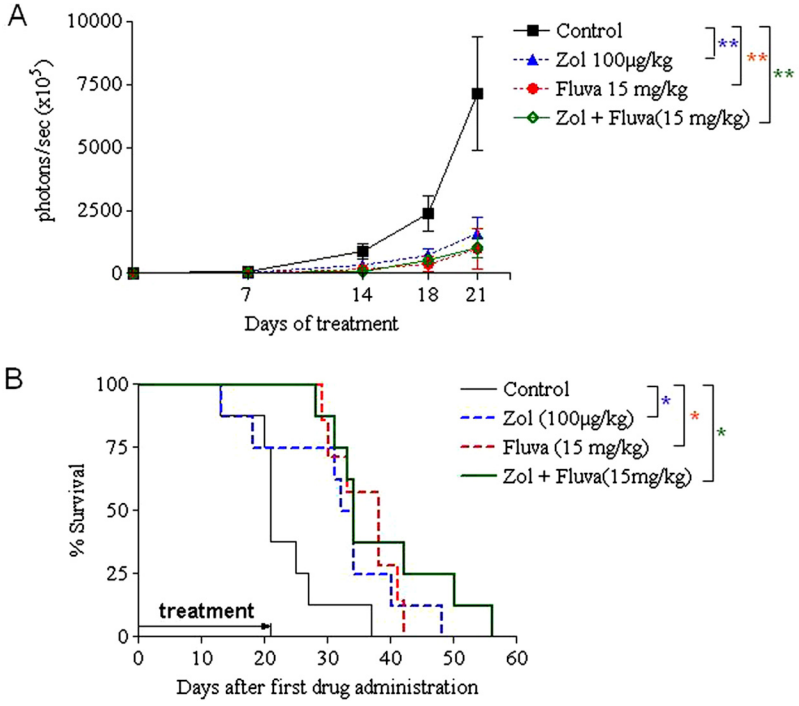

Fig. 5. Effect of the Fluva and Zol combination in vivo. Bioluminescent MDA-MB-231 (D3H2LN) cells (10^5) were injected into the left ventricle of nude mice. Only mice with successful intracardiac injection of cells, witnessed by an overall luminescent signal, continued the experiment. As described in the legend to Fig. 2, mice were treated upon detection of established metastasis (referred to as day 0) with Zol (at 100 μg/kg three times a week), Fluva (at 15 mg/kg daily), their combination (100 μg/kg Zol three time a week + 15 mg/kg Fluva daily), or PBS (daily for control group) during 3 weeks. A, plot of bioluminescent signal; each point represents a mean (± S.E.M.) signal of eight (control, Zol, Fluva, or Zol with Fluva combination) or seven (Fluva) mice. **, $P < 0.01$ versus control [ANOVA Tukey-Kramer multiple comparisons test for day 21 control, Zol, Fluva (15mg/kg), and Zol + Fluva (15 mg/kg)]. *B,* Kaplan-Meyer survival curves for control and treated mice (median survival of 21 days for control and 33, 38, and 34 days for Zol, Fluva, and the Zol with Fluva combination, respectively) generated for the 3-week treatment period and followed up until they died. *, $P < 0.05$.

with the highest Fluva concentration (15 mg/kg) did not significantly change the level of the bioluminescence metastasis signal (Fig. 5A) or the number of metastatic sites (data not shown) compared with Zol or Fluva alone. Survival analysis showed no significant differences between Zol, Fluva (at 15 mg/kg), or their combination (Fig. 5B), with median sur-

vival of 33, 38, and 34 days, respectively. Moreover, combinatorial treatment did not result in any improvement of the effect seen with Fluva when administered at a nonefficient 1 mg/kg concentration (Supplemental Fig. S1).

Discussion

For the first time, we demonstrate the curative effect of Fluva on breast cancer metastases in vivo using the MDA-MB-231 population (D3H2LN) metastasis model. Indeed, Fluva induces a strong inhibition of the progression of established metastases (80%) when administered at 15 mg/kg. Compared with Zol, Fluva alone delayed the growth of established metastases as soon as the 1st week of the treatment. We observed a partial metastasis regression in three of seven mice characterized by decay of bioluminescent signal. However, this effect was not observed in all mice because we only detected 40% of inhibition in the mean number of metastasis sites (data not shown). With regard to organs affected by metastases, both Zol and Fluva affected localization of both bone and visceral metastases.

Transcriptomic analyses of MDA-MB-231 cells treated with Fluva or Zol demonstrate common regulation of genes implicated in metastatic capacities of tumor cells. The majority of differentially expressed genes with 12 and 24-h Fluva (2 μM for $IC_{50\ 72\ h}$ concentration) treatment were regulated in the same manner by Zol when incubated at its $IC_{50\ 72\ h}$ (30 μM) for a longer time (48 h) or with a higher concentration (100 μM) for the same treatment time (24 h). This kinetic difference between proliferation and transcriptomic activity could be explained by the higher lipophilicity of Fluva versus Zol (logP 3.69 versus -0.93, respectively), which allowed better penetration of Fluva into the cells. In addition, proliferation might involve protein post-translational changes that cannot be directly evaluated in transcriptome analysis. Genes implicated in cellular movement, cellular growth and proliferation, and development as well as apoptosis are regulated in the same manner and provide target metastatic genes for both molecules. For instance, gene expression is consistent with the proapoptotic activity of both drugs: the expression of 14 proapoptotic genes (*TP53INP1*, *BTG1*, *TNS4*, *PGEP1*, *TP5313*, *MAP3K5*, *BINP3L*, *IFIH1*, *IER3*, *PTPRH*, *TMEM173*, *SLK,CD14*, and *TNFRSF1A*) is increased, whereas only 6 proapoptotic genes are down-regulated (*TGM2*, *ERCC2*, *PAWR*, *AEN*, *TNFRSF12A*, and *FAM176A*).

Some genes modified by both drugs are also involved in immune and inflammatory responses. Genes modulating the immune response are up-regulated when they stimulate the immune system (*CMKLR1*, *APOBE3CF*, *TLR6*, *REG*, *IFIH1*, *ANXA11*, *TMEM173*, and *CD14*) and down-regulated when they are immunosuppressive (*PTGER4*, *PDCD1LG2*, and *CD174*), attributing globally to both drugs an immunostimulant profiles. This effect of Fluva on cancer cells is notably different from what is observed in immune cells, in which statins inhibit the immune system (Greenwood et al., 2006). This point is important because it demonstrates that these molecules could interact in concert with the immune system to induce suppression of cancer cells. To verify this finding, it would be interesting to further study drug effects on processes of metastases in an immunocompetent mice model.

Only one in vivo study of statins combined with bisphosphonates showed a delay in pancreatic tumor growth and an increase in mouse survival when lovastatin and pamidronate were combined (Issat et al., 2007). In addition, Fluva alone or in association with other drugs has been reported to inhibit tumor growth and formation of metastases in hepatocarcinoma cell lines (Paragh et al., 2003; Issat et al., 2007). In addition, Fluva is effective on other cancers such as pancreatic and head and neck carcinomas (Bocci et al., 2005; Fujiwara et al., 2008). For breast cancer cells, the use of Fluva in combination with other chemotherapeutic molecules was also described in vitro (Budman et al., 2007), lacking in vivo data. In our in vivo study of Fluva, we observed no differences in metastatic growth in combination treatments. Association of Fluva and Zol at their efficient concentrations (15 mg/kg and 100 μg/kg, respectively) resulted in no significant differences compared with the effects of these drugs alone as also seen for combination treatment with Fluva at a nonefficient 1 mg/kg concentration. Observation of common transcriptomic profiles between Zol and Fluva supported this finding of the absence of synergy in vivo. The differences observed between our work on metastasis and that of others on tumor xenografts can also be explained by these molecule activities because they both target Rho/Ras proteins. However, in regard to genes whose expression depends on prenylation of Ras protein or Rho activation (Bild et al., 2006), only 9% of the total number of these genes were modified by Zol or Fluva. This finding suggested that other mechanisms are involved in the inhibition of metastasis formation by the two drugs. Furthermore, the specific capacity of Zol to inhibit DNA synthesis could complete with that of Fluva in the primary tumor rather than in metastatic cell growth.

In conclusion, this study demonstrates the potential benefit of the use of Fluva associated or not associated with bisphosphonates in the context of established breast cancer metastases. It also suggests that the frequent association of statins and bisphosphonates in older patients could influence the course of breast metastasis.

Acknowledgments

We thank N. Setterblat and C. Doliger for excellent technical support.

Authorship Contributions

Participated in research design: Vintonenko, Perret, Crepin, and Di Benedetto

Conducted experiments: Vintonenko, Kassis, and Abdelkarim.

Contributed new reagents or analytic tools: Lecouvey.

Performed data analysis: Vintonenko, Jais, and Di Benedetto.

Wrote or contributed to the writing of the manuscript: Vintonenko, Jais, Perret, and Di Benedetto.

References

Aapro M, Abrahamsson PA, Body JJ, Coleman RE, Colomer R, Costa L, Crinò L, Dirix L, Gnant M, Gralow J, et al. (2008) Guidance on the use of bisphosphonates in solid tumours: recommendations of an international expert panel. *Ann Oncol* **19:**420–432.

Ahern TP, Pedersen L, Tarp M, Cronin-Fenton DP, Garne JP, Silliman RA, Sørensen HT, and Lash TL (2011) Statin prescriptions and breast cancer recurrence risk: a Danish nationwide prospective cohort study. *J Natl Cancer Inst* 103:1461–1468.

Bild AH, Yao G, Chang JT, Wang Q, Potti A, Chasse D, Joshi MB, Harpole D, Lancaster JM, Berchuck A, et al. (2006) Oncogenic pathway signatures in human cancers as a guide to targeted therapies. *Nature* **439:**353–357.

Bocci G, Fioravanti A, Orlandi P, Bernardini N, Collecchi P, Del Tacca M, and Danesi R (2005) Fluvastatin synergistically enhances the antiproliferative effect of gemcitabine in human pancreatic cancer MIAPaCa-2 cells. *Br J Cancer* **93:**319–330.

Budman DR and Calabro A (2006) Zoledronic acid (Zometa) enhances the cytotoxic effect of gemcitabine and fluvastatin: in vitro isobologram studies with conventional and nonconventional cytotoxic agents. *Oncology* **70:**147–153.

Budman DR, Tai J, and Calabro A (2007) Fluvastatin enhancement of trastuzumab and classical cytotoxic agents in defined breast cancer cell lines in vitro. *Breast Cancer Res Treat* **104:**93–101.

Campbell MJ, Esserman LJ, Zhou Y, Shoemaker M, Lobo M, Borman E, Baehner F, Kumar AS, Adduci K, Marx C, et al. (2006) Breast cancer growth prevention by statins. *Cancer Res* **66:**8707–8714.

Caraglia M, Santini D, Marra M, Vincenzi B, Tonini G, and Budillon A (2006) Emerging anti-cancer molecular mechanisms of aminobisphosphonates. *Endocr Relat Cancer* **13:**7–26.

Cauley JA, McTiernan A, Rodabough RJ, LaCroix A, Bauer DC, Margolis KL, Paskett ED, Vitolins MZ, Furberg CD, Chlebowski RT, et al. (2006) Statin use and breast cancer: prospective results from the Women's Health Initiative. *J Natl Cancer Inst* **98:**700–707.

Denoyelle C, Hong L, Vannier JP, Soria J, and Soria C (2003) New insights into the actions of bisphosphonate zoledronic acid in breast cancer cells by dual RhoA-dependent and -independent effects. *Br J Cancer* **88:**1631–1640.

Dudakovic A, Wiemer AJ, Lamb KM, Vonnahme LA, Dietz SE, and Hohl RJ (2008) Inhibition of geranylgeranyl diphosphate synthase induces apoptosis through multiple mechanisms and displays synergy with inhibition of other isoprenoid biosynthetic enzymes. *J Pharmacol Exp Ther* **324:**1028–1036.

Duivenvoorden WC, Vukmirović-Popović S, Kalina M, Seidlitz E, and Singh G (2007) Effect of zoledronic acid on the doxycycline-induced decrease in tumour burden in a bone metastasis model of human breast cancer. *Br J Cancer* **96:**1526–1531.

Edgar R, Domrachev M, and Lash AE (2002) Gene Expression Omnibus: NCBI gene expression and hybridization array data repository. *Nucleic Acids Res* **30:**207–210.

Fournier PG, Stresing V, Ebetino FH, and Clézardin P (2010) How do bisphosphonates inhibit bone metastasis in vivo? *Neoplasia* **12:**571–578.

Fritz G, Just I, and Kaina B (1999) Rho GTPases are over-expressed in human tumors. *Int J Cancer* **81:**682–687.

Fujiwara K, Tsubaki M, Yamazoe Y, Nishiura S, Kawaguchi T, Ogaki M, Nishinobo M, Shimamoto K, Moriyama K, and Nishida S (2008) Fluvastatin induces apoptosis on human tongue carcinoma cell line HSC-3. *Yakugaku Zasshi* **128:**153–158.

Green J, Gschaidmeier H, Yoneda T, and Mundy G (2000) Zoledronic acid potently inhibits tumour-induced osteolysis in two models of breast cancer metastasis to bone. *Ann Oncol* **11:**14.

Greenwood J, Steinman L, and Zamvil SS (2006) Statin therapy and autoimmune disease: from protein prenylation to immunomodulation. *Nat Rev Immunol* **6:**358–370.

Hamma-Kourbali Y, Di Benedetto M, Ledoux D, Oudar O, Leroux Y, Lecouvey M, and Kraemer M (2003) A novel non-containing-nitrogen bisphosphonate inhibits both in vitro and in vivo angiogenesis. *Biochem Biophys Res Commun* **310:**816–823.

Hiraga T, Williams PJ, Ueda A, Tamura D, and Yoneda T (2004) Zoledronic acid inhibits visceral metastases in the 4T1/luc mouse breast cancer model. *Clin Cancer Res* **10:**4559–4567.

Irizarry RA, Hobbs B, Collin F, Beazer-Barclay YD, Antonellis KJ, Scherf U, and Speed TP (2003) Exploration, normalization, and summaries of high density oligonucleotide array probe level data. *Biostatistics* **4:**249–264.

Issat T, Nowis D, Legat M, Makowski M, Klejman MP, Urbanski J, Skierski J, Koronkiewicz M, Stoklosa T, Brzezinska A, et al. (2007) Potentiated antitumor effects of the combination treatment with statins and pamidronate in vitro and in vivo. *Int J Oncol* **30:**1413–1425.

Istvan E (2003) Statin inhibition of HMG-CoA reductase: a 3-dimensional view. *Atheroscler Suppl* **4:**3–8.

Jadhav SB and Jain GK (2006) Statins and osteoporosis: new role for old drugs. *J Pharm Pharmacol* **58:**3–18.

Jagdev SP, Coleman RE, Shipman CM, Rostami-H A, and Croucher PI (2001) The bisphosphonate, zoledronic acid, induces apoptosis of breast cancer cells: evidence for synergy with paclitaxel. *Br J Cancer* **84:**1126–1134.

Jenkins DE, Hornig YS, Oei Y, Dusich J, and Purchio T (2005) Bioluminescent human breast cancer cell lines that permit rapid and sensitive in vivo detection of mammary tumors and multiple metastases in immune deficient mice. *Breast Cancer Res* **7:**R444–R454.

Kozma SC, Bogaard ME, Buser K, Saurer SM, Bos JL, Groner B, and Hynes NE (1987) The human c-Kirsten ras gene is activated by a novel mutation in codon 13 in the breast carcinoma cell line MDA-MB231. *Nucleic Acids Res* **15:**5963–5971.

Kusama T, Mukai M, Tatsuta M, Nakamura H, and Inoue M (2006) Inhibition of transendothelial migration and invasion of human breast cancer cells by preventing geranylgeranylation of Rho. *Int J Oncol* **29:**217–223.

Lecouvey M, Mallard I, Burgada R, and Leroux Y (2001) A mild and efficient one-pot synthesis of 1-hydroxymethylene-1,1-bisphosphonic acids. Preparation of new tripod ligands. *Tetrahedron Lett* **42:**8475–8478.

Loboda A, Nebozhyn M, Klinghoffer R, Frazier J, Chastain M, Arthur W, Roberts B, Zhang T, Chenard M, Haines B, et al. (2010) A gene expression signature of RAS pathway dependence predicts response to PI3K and RAS pathway inhibitors and expands the population of RAS pathway activated tumors. *BMC Med Genomics* **3:**26.

Mönkkönen H, Auriola S, Lehenkari P, Kellinsalmi M, Hassinen IE, Vepsäläinen J, and Mönkkönen J (2006) A new endogenous ATP analog (ApppI) inhibits the mitochondrial adenine nucleotide translocase (ANT) and is responsible for the apoptosis induced by nitrogen-containing bisphosphonates. *Br J Pharmacol* **147:**437–445.

Monteil M, Guenin E, Migianu E, Lutomski D, and Lecouvey M (2005) Bisphosphonate prodrugs: synthesis of new aromatic and aliphatic 1-hydroxy-1,1-bisphosphonate partial esters. *Tetrahedron* **61:**7528–7537.

Mosmann T (1983) Rapid colorimetric assay for cellular growth and survival: application to proliferation and cytotoxicity assays. *J Immunol Methods* **65:**55–63.

Paragh G, Kertai P, Kovacs P, Paragh G Jr, Fülöp P, and Foris G (2003) HMG CoA reductase inhibitor fluvastatin arrests the development of implanted hepatocarcinoma in rats. *Anticancer Res* **23:**3949–3954.

Peyruchaud O, Winding B, Pécheur I, Serre CM, Delmas P, and Clézardin P (2001) Early detection of bone metastases in a murine model using fluorescent human breast cancer cells: application to the use of the bisphosphonate zoledronic acid in the treatment of osteolytic lesions. *J Bone Miner Res* **16:**2027–2034.

Pfaffl MW, Horgan GW, and Dempfle L (2002) Relative expression software tool (REST) for group-wise comparison and statistical analysis of relative expression results in real-time PCR. *Nucleic Acids Res* **30:**e36.

Reinholz GG, Getz B, Sanders ES, Karpeisky MY, Padyukova NSh, Mikhailov SN, Ingle JN, and Spelsberg TC (2002) Distinct mechanisms of bisphosphonate action between osteoblasts and breast cancer cells: identity of a potent new bisphosphonate analogue. *Breast Cancer Res Treat* **71:**257–268.

Russell RG (2011) Bisphosphonates: the first 40 years. *Bone* **49:**2–19.

Senaratne SG, Mansi JL, and Colston KW (2002) The bisphosphonate zoledronic acid impairs Ras membrane [correction of impairs membrane] localisation and induces cytochrome c release in breast cancer cells. *Br J Cancer* **86:**1479–1486.

Yano S, Zhang H, Hanibuchi M, Miki T, Goto H, Uehara H, and Sone S (2003) Combined therapy with a new bisphosphonate, minodronate (YM529), and chemotherapy for multiple organ metastases of small cell lung cancer cells in severe combined immunodeficient mice. *Clin Cancer Res* **9:**5380–5385.

Address correspondence to: Dr. M. Di Benedetto, INSERM UMRS 940, IGM 27 rue Juliette Dodu, France. E-mail: dibenedetto22@yahoo.fr